3D-QSAR Model of Flavonoids Binding at Benzodiazepine Site in GABA$_A$ Receptors

Xiaoqin Huang,[†,‡] Tong Liu,[†] Jiande Gu,[†] Xiaomin Luo,[†] Ruyun Ji,[†] Yang Cao,[§] Hong Xue,*,[‖] J. Tze-Fei Wong,[‖] Bing L. Wong,[⊥] Gang Pei,[‡] Hualiang Jiang,*,[†] and Kaixian Chen[†]

Center for Drug Discovery and Design, State Key Laboratory of Drug Research, Shanghai Institute of Materia Medica, Shanghai Institutes for Biological Sciences, Chinese Academy of Sciences, 294 Taiyuan Road, Shanghai 200031, P. R. China, Shanghai Institute of Biological Chemistry and Cell Biology, Shanghai Institutes for Biological Sciences, Chinese Academy of Sciences, 320 Yueyang Road, Shanghai 200032, Suzhou University, Suzhou 215006, P. R. China, Department of Biochemistry, Hong Kong University of Science & Technology, Hong Kong, P. R. China, and Naturon Limited, 353 Lockhart Road, Wanchai, Hong Kong, P. R. China

With flavone as a structural template, three-dimensional quantitative structure–activity relationship (3D-QSAR) studies and ab initio calculations were performed on a series of flavonoids. A reasonable pharmacophore model was built through CoMFA, CoMSIA, and HQSAR analyses and electrostatic potential calculations. A plausible binding mode for flavonoids with GABA$_A$ receptors was rationalized. On the basis of the commonly recognized binding site, the specific S1 and S2 subsites relating to substituent positions were proposed. The different binding affinities could be explained according to the frontier orbitals and electrostatic potential (ESP) maps. The ESP could be used as a novel starting point for designing more selective BZ-binding-site ligands.

Introduction

Flavonoids,[1] first isolated from an herb plant that was used as tranquilizers in folkloric medicine, have been shown to possess a selective and relatively mild affinity for the benzodiazepine binding site of GABA$_A$ receptors (BZRs).[2–4] This new family of natural products, along with various synthetic derivatives,[5] has an extremely potent anxiolytic effect, which is not associated with myorelaxant, amnestic, or sedative actions.[6] These findings have prompted a search for high-affinity ligands with anxioselective properties.[7] For example, introduction of bromine at position 6 (Table 1) of flavone resulted in a more than 10-fold increase in the binding affinity.[8] 6-Bromoflavone has a GABA ratio of 1.6–2.0 and a pharmacological profile similar to that of diazepam, a full agonist. Even more potent ligands have been obtained by the introduction of nitro groups. 6,3′-Dinitroflavone exhibits K_i values ranging from 17 to 50 nM[4] with a slight preference for BZ$_1$ sites and is an extremely potent anxiolytic lacking muscle relaxation effects. 6-Bromo-3′-nitroflavone shows a slightly increased affinity for the BZRs compared to the dinitro analogues, and it also exhibits moderate selectivity for the BZ$_1$ sites. The anxiolytic effect of this compound is lower than that of 6,3′-dinitroflavone but is still comparable to that of diazepam.

Because of their selective pharmacological profile and low intrinsic efficacy to BZRs, flavonoid derivatives represent an improved therapeutic tool in the treatment of anxiety and have been important leads for the development of potent and selective BZR ligands.[9] A number of BZR-binding-site pharmacophore models,[10,11] as well as structure–activity relationships (SARs),[12–14] have been proposed on the basis of synthesis and computer-assisted analysis. These models have defined the structural requirements needed for high binding affinity of ligands to BZRs and therefore offered some beneficial clues in structural modifications for medicinal chemists. Considering these models, it is still necessary to study three-dimensional quantitative relationships (3D-QSAR) of flavonoids. Accordingly, we have performed molecular modeling studies on a series of flavonoids using the comparative molecular fields analysis (CoMFA),[15] comparative molecular similarity analysis (CoMSIA),[16] and hologram QSAR (HQSAR) approaches,[17] as well as ab initio quantum chemistry methods.[18] The results from these studies may be helpful to develop valid and predictive models for novel ligand design.

Computational Details

A series of 38 flavonoid molecules were employed in all the calculations (Table 1). The initial structures of these compounds were built on the basis of the structure of flavone. All the calculations were performed on a Silicon Graphics Indigo XZ R10000 workstation, using Sybyl 6.5[19] and Gaussian 98.[18]

1. Conformational Searching and Molecular Alignment. A systematic conformational search for flavonoid molecules was performed, the torsion angle increment during the conformational search was set to 10° in the range 0–360°, and the flexibility of all the torsion angles was considered. The local minimum-energy conformations, including the lowest-energy conformation, of each molecule were obtained. These conformations were further refined by molecular mechanics using Tripos force field and Gasteiger–Hückel charges; a nonbond cutoff of 8 Å was adopted in the structural optimization to consider the intramolecular interactions.

* To whom correspondence should be addressed. For Prof. Hualiang Jiang: phone, +86-21-64311833, ext 222; fax: +86-21-64370269; e-mail, hljiang@mail.shcnc.ac.cn; jiang@iris3.simm.ac.cn. For Prof. Hong Xue: e-mail, hxue@ust.hk.
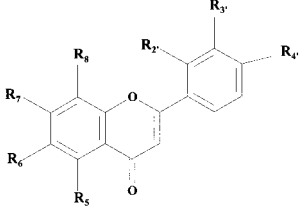† Shanghai Institute of Materia Medica, Shanghai Institutes for Biological Sciences.
‡ Shanghai Institute of Biological Chemistry and Cell Biology, Shanghai Institutes for Biological Sciences.
§ Suzhou University.
‖ Hong Kong University of Science & Technology.
⊥ Naturon Limited.

Table 1. Compounds in This Study and Their BZ Site Binding Affinities ($-\log K_i$, K_i in nM)

compd	R_5	R_6	R_7	R_8	$R_{2'}$	$R_{3'}$	$R_{4'}$	$-\log K_i$
1	−H	−H	−H	−H	−H	−H	−H	6.00
2	−H	−F	−H	−H	−H	−OH	−H	5.60
3	−H	−Cl	−H	−H	−H	−OH	−H	6.07
4	−H	−Br	−H	−H	−H	−OH	−H	6.22
5	−H	−F	−H	−H	−H	−NO$_2$	−H	6.74
6	−H	−Cl	−H	−H	−H	−NO$_2$	−H	8.10
7	−H	−Cl	−H	−H	−H	−H	−OCH$_3$	5.90
8	−H	−Br	−H	−H	−H	−H	−OCH$_3$	5.68
9	−H	−Br	−H	−H	−NO$_2$	−H	−H	6.68
10	−H	−NO$_2$	−H	−H	−H	−H	−Br	7.60
11	−H	−Cl	−H	−H	−F	−H	−H	6.38
12	−H	−Br	−H	−H	−F	−H	−H	6.42
13	−H	−H	−H	−H	−H	−F	−H	5.45
14	−H	−F	−H	−H	−H	−F	−H	6.04
15	−H	−Cl	−H	−H	−H	−F	−H	6.93
16	−H	−Br	−H	−H	−H	−F	−H	7.38
17	−H	−H	−H	−H	−H	−H	−F	5.44
18	−H	−F	−H	−H	−H	−H	−F	5.60
19	−H	−Cl	−H	−H	−H	−H	−F	6.74
20	−H	−Br	−H	−H	−H	−H	−F	6.94
21	−H	−H	−H	−H	−H	−Cl	−H	6.21
22	−H	−F	−H	−H	−H	−Cl	−H	6.70
23	−H	−Cl	−H	−H	−H	−Cl	−H	7.64
24	−H	−Br	−H	−H	−H	−Cl	−H	7.77
25	−H	−H	−H	−H	−H	−Br	−H	6.38
26	−H	−F	−H	−H	−H	−Br	−H	6.63
27	−H	−Cl	−H	−H	−H	−Br	−H	7.64
28	−H	−Br	−H	−H	−H	−Br	−H	7.72
29	−H	−Br	−H	−H	−H	−H	−H	7.15
30	−H	−Br	−H	−H	−H	−H	−NO$_2$	6.70
31	−H	−NO$_2$	−H	−H	−H	−NO$_2$	−H	7.92
32	−H	−Br	−H	−H	−H	−NO$_2$	−H	9.00
33	−OH	−Br	−OH	−Br	−H	−H	−H	6.15
34	−OH	−H	−OH	−H	−H	−H	−H	5.52
35	−OH	−H	−OH	−H	−H	−H	−OH	5.52
36	−OH	−H	−OH	−H	−Cl	−H	−H	5.10
37	−OH	−H	−OH	−H	−F	−H	−H	5.10
38	−OH	−OCH$_3$	−OH	−H	−H	−H	−OH	6.00
baicalin[a]	−OH	−OH	−C$_6$H$_9$O$_7$[b]	−H	−H	−H	−H	4.11
baicalein[a]	−OH	−OH	−OH	−H	−H	−H	−H	5.25
scutellarein[a]	−OH	−OH	−OH	−H	−H	-H	−OH	4.92
wogonin[a]	−OH	−H	−OH	−OCH$_3$	−H	−H	−H	5.69

[a] Compounds that were not included in the training set of compounds in 3D-QSAR model. [b] −C$_6$H$_9$O$_7$ = 5−carboxyglucosyloxy.
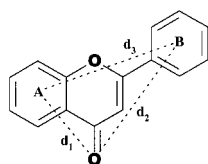
Figure 1. Alignment rules for flavonoids. A and B are the pseudoatoms representing the centers of the two aromatic rings in the structure of flavonoids. d_1, d_2, and d_3 are the distances between three key moieties of flavonoid molecules.

Conformational alignment was carried out by taking the centers of aromatic rings A and B (pseudoatoms A and B in Figure 1) and the oxygen atom of carboxide as the atomic pairs. These key moieties of flavonoid molecules were the components of the pharmacophore, so the distances between them, d_1, d_2, and d_3 (Figure 1), were also taken into account in the conformational superimposition.

2. 3D-QSAR Studies. 2.1. CoMFA. For the CoMFA calculations, steric and electrostatic field energies were calculated using sp^3 carbon as the steric probe atom and a +1 net charge as the electrostatic probe. Steric and electrostatic interactions were calculated using the Tripos force field with a distance-dependent dielectric constant $\epsilon = 1r$ at all intersections in a regularly spaced (2 Å) grid. The cutoff was set to 30 kcal/mol. The minimum σ (column filtering) was set to 2.0 kcal/mol to improve the signal-to-noise ratio by omitting those lattice points whose energy variation was below this threshold. Regression analysis was performed using the cross validation of compounds leave-one-out method. The optimal number of components used in the non-cross-validation (conventional) analysis was defined as that which yielded the highest cross-validated r^2 value. Cross-validation analyses were performed for all sets of the local minimum-energy conformations derived from the conformational search. The conformation set corresponding to the highest cross-validated r^2 value was selected for further non-cross-validation analysis. For component models with identical values, the component number producing the smallest standard error of prediction (SEP) was selected.

2.2. CoMSIA. The CoMFA alignment also served to compute steric, electrostatic, and hydrophobic similarity index fields for CoMSIA.[16] The steric contribution was reflected by the third power of the atomic radii of the atoms. Electrostatic properties were introduced as Gasteiger−Hückel charges. An atom-based hydrophobicity was assigned according to the parametrization developed by Viswanadhan et al.[20] The lattice dimensions were selected with a sufficiently large margin (> 4 Å) to enclose all aligned molecules. The advantage of CoMSIA[16] fields is that no singularities occurred at atomic positions due to Gaussian-type distance dependence of the physicochemical properties. Thus, no arbitrary cutoffs were required. Similarity indexes were computed using a probe with a charge of +1, a radius of +1, a hydrophobicity of +1, and 0.3 as an attenuation factor α for the Gaussian-type distance. The statistical evaluation for the CoMSIA analysis was carried out in the same way as described in CoMFA.

2.3. HQSAR. The following procedure was used to construct molecular holograms containing the HQSAR descriptors. First, the molecule was hashed to a molecular fingerprint that encoded the frequency of occurrence of various molecular fragment types using a predefined set of rules. This molecular fingerprint was cut into strings at a fixed interval as specified by a hologram length (HL) parameter. All generated strings were then hashed into a fixed-length array to produce the molecular hologram. During this process, the Sybyl line notation (SLN) for each string generated was mapped to a unique integer in the range $0-2^{31}$ using a cyclic redundancy check (CRC) algorithm. The numerical representation of molecules was exploited by a subsequent correlation analysis; typically a partial least-squares (PLS) QSAR model was constructed. The optimal HQSAR model was derived from screening through the 12 default HL values, which were a set of 12 prime numbers ranging from 53 to 401.

3. Ab Initio Calculations. Two representative compounds, flavone (**1**) and 6-bromo-3′-nitroflavone (**32**), which have the highest binding affinity among the 38 compounds, were calculated with the ab initio Hartree−Fock SCF method along with the standard polarized double-ζ basis set (6-31G**). Usually, molecular properties could be calculated by performing single-point calculations with ab initio methods based on the structures optimized by molecular mechanics. However, the conformation should be optimized by the SCF method during the ab initio calculation to get more reasonable results of molecular orbitals and molecular electrostatic potential. All the torsion angles were constrained on the conformation derived from the conformation search during the ab initio calculations. Accordingly, the geometry of these two compounds had been optimized with torsion angle constraints at the HF/6-31G** level based on the conformation set having the highest cross-validated r^2 value. The highest-occupied molecular orbital (HOMO), the lowest-unoccupied molecular orbital (LUMO), and the electrostatic potentials (ESP) were precisely calculated. To obtain the binding difference between flavonoids and other BZ ligands, same quantum chemical calculations were performed on diazepam. Full geometric optimizations were also performed using HF/6-31G** method on compounds **1** and **32** in order to address the fluctuation between the binding conformations and the local energy minima.

Results and Discussion

1. CoMFA, CoMSIA, and HQSAR Analyses. 1.1. CoMFA. The major objective when working with CoMFA analysis is to find the best predictive model within the system. PLS analysis results based on a least-squares fit are listed in Table 2, which shows that all the statistical indexes are reasonably high. Table 3 shows the data of the predicted $-\log K_i$ values vs the experimental results. Figure 2a represents the relationship between the experimental binding affinities ($-\log K_i$) and the predicted activities by the CoMFA

Table 2. CoMFA Result for the Flavonoids

leave-one-out		cross-validated		conventional		
n_{leave}^2	optimal components	r_{cross}^2	optimal components	r^2	s	F
0.752	4	0.745	5	0.969	0.165	174.594

contributions	
steric	electrostatic
0.535	0.465

Table 3. Predicted Activities (PA) vs Experimental Activities (EA) and the Residues (δ) of CoMFA, CoMSIA, and HQSAR

compd	EA	CoMFA PA	CoMFA δ	CoMSIA PA	CoMSIA δ	HQSAR PA	HQSAR δ
1	6.00	5.87	0.13	5.92	0.08	6.10	−0.10
2	5.60	5.26	0.34	5.42	0.18	5.72	−0.12
3	6.07	6.25	−0.18	5.90	0.17	5.89	0.18
4	6.22	6.39	−0.17	6.28	−0.06	6.10	0.12
5	6.74	6.89	−0.15	6.80	−0.06	6.60	0.14
6	8.10	7.82	0.28	7.90	0.20	8.25	−0.15
7	5.90	5.77	0.13	6.02	−0.12	5.73	0.17
8	5.68	5.90	−0.22	5.78	−0.10	5.50	0.18
9	6.68	6.67	0.01	6.73	0.05	6.75	−0.07
10	7.60	7.41	0.19	7.52	0.08	7.80	−0.20
11	6.38	6.30	0.08	6.50	−0.12	6.21	0.17
12	6.42	6.43	−0.01	6.45	−0.03	6.40	0.02
13	5.45	5.57	−0.12	5.48	−0.03	5.15	0.30
14	6.04	6.13	−0.09	5.93	0.11	6.15	−0.11
15	6.93	6.87	0.06	6.81	0.12	6.78	0.15
16	7.38	7.00	0.38	7.20	0.18	7.48	−0.10
17	5.44	5.49	−0.05	5.46	−0.02	5.50	−0.06
18	5.60	5.81	−0.21	5.40	0.20	5.71	−0.11
19	6.74	6.79	−0.05	6.70	0.04	6.80	−0.06
20	6.94	6.92	0.02	7.10	−0.16	6.80	0.14
21	6.21	6.13	−0.09	6.05	0.16	6.32	−0.11
22	6.70	6.64	0.06	6.80	−0.10	6.77	−0.07
23	7.64	7.62	0.02	7.51	0.13	7.72	−0.08
24	7.77	7.80	−0.03	7.89	−0.09	7.88	−0.11
25	6.38	6.33	0.05	6.48	−0.10	6.28	0.10
26	6.63	6.64	−0.01	6.65	−0.02	6.58	0.05
27	7.64	7.63	0.01	7.72	−0.08	7.60	0.04
28	7.72	7.76	−0.04	7.80	−0.08	7.66	0.06
29	7.15	7.26	−0.11	7.02	0.13	7.10	0.05
30	6.70	6.67	0.03	6.83	−0.13	6.77	−0.07
31	7.92	8.07	−0.15	8.10	−0.18	7.81	0.11
32	9.00	8.92	0.08	9.10	−0.10	9.08	−0.08
33	6.15	6.18	−0.03	6.25	−0.10	6.10	0.05
34	5.52	5.60	−0.08	5.58	−0.06	5.45	0.07
35	5.52	5.50	0.02	5.56	−0.04	5.44	0.08
36	5.10	5.09	0.01	5.04	0.06	5.15	−0.05
37	5.10	5.04	0.06	5.06	0.04	5.20	−0.10
38	6.00	5.95	0.05	6.05	−0.05	5.85	0.15
baicalin[a]	4.11	4.54	−0.43	4.30	−0.20	4.21	−0.10
baicalein[a]	5.25	5.63	−0.38	5.04	0.21	5.50	−0.25
scutellarein[a]	4.92	4.86	0.06	5.01	−0.09	5.10	−0.18
wogonin[a]	5.69	6.04	−0.35	5.83	−0.14	5.55	0.14

[a] Compounds that were not included in the training set of the 3D-QSAR model.

model. All of these results indicate that the CoMFA model has a fair predictive ability.

The QSAR produced by CoMFA, which is usually represented as a 3D "coefficient contour", is shown in Figure 3. Beneficial and detrimental steric interactions are displayed in green and yellow contours, respectively, while red and blue contours illustrate regions of desirable negative and positive electrostatic interactions. Taken together with the structural characteristics of flavonoids, several important regions of the binding site can readily be observed from Figure 3. Some large regions of green contour near position 6 (Figure 3a)
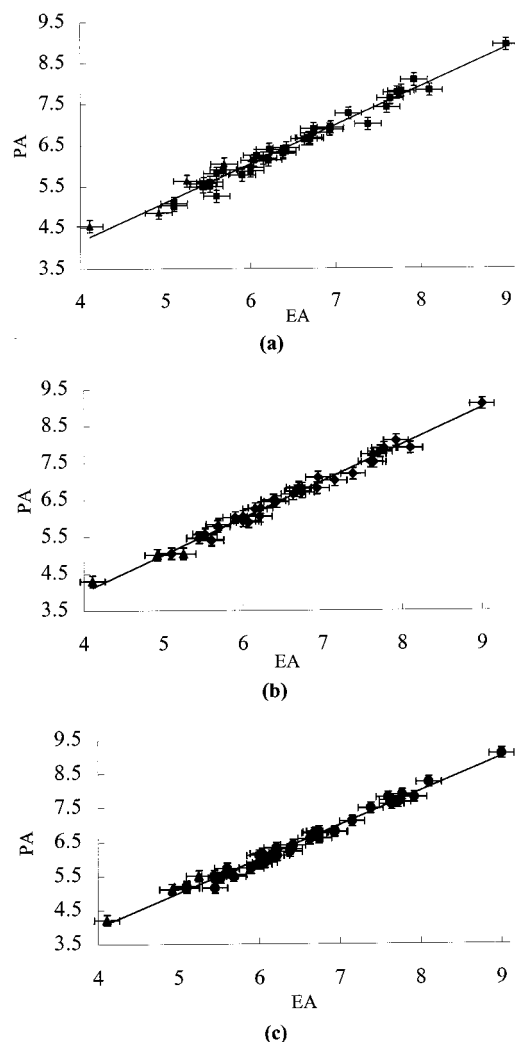
Figure 2. Relationship between predicted binding affinities (PA) from CoMFA (a), CoMSIA (b), and HQSAR (c) models and the experimental $-\log K_i$ values (EA) of flavonoids. ▲: Testing compounds that were not included in the training set of QSAR analyses. The standard error of prediction is also shown for each compound

Figure 3. CoMFA contour maps: (a) steric contributions to the binding affinities of flavonoids; (b) electrostatic contributions to the binding affinities of flavonoids.

Table 4. CoMSIA Result for the Flavonoids

	cross-validated		conventional		
descriptors	r_{cross}^2	optimal components	r^2	s	F
steric (S)	0.553	6	0.862	0.374	32.222
electrostatic (E)	0.285	2	0.744	0.509	15.008
electrostatic + steric	0.436	2	0.855	0.383	30.485
HB acceptor (A)	0.372	2	0.496	0.715	5.088
acceptor + donor	0.139	2	0.550	0.690	6.525
hydrophobic (H)	0.249	5	0.850	0.390	29.316
S + E + A + H	0.733	5	0.948	0.219	110.482

contributions			
steric	electrostatic	hydrophobic	HB acceptor
0.281	0.341	0.233	0.155

suggest that more bulky substituents at this position will significantly improve the affinity. The yellow polyhedron near positions 5 and 7 and aromatic ring B indicate that more steric bulk is unfavorable for the binding affinity. The blue contour near positions 6 and 7 (Figure 3b) suggests that negatively charged substituents could increase the activity. The red polyhedrons near position 3′ indicate that low electron density or the ability of substituents to draw electrons at position 3′ might play a favorable role in binding affinity. Accordingly, the compounds with substituents at position 6 have higher $-\log K_i$ values than the compounds without substituents at this position. As the van der Waals radius and the ability to elevate electronic density of the substituents increase, the binding affinities become higher. The effectiveness of increasing the binding affinities of different substituents at position 6 is in the sequence Br > Cl > NO₂ > F. The addition of a bulky group or the presence of a negatively charged hydroxyl group at position 7 is not beneficial to the binding affinity, and this may be the reason that the $-\log K_i$ values of compounds **33−38** and baicalin (Table 1) are lower than those of other compounds. Hydroxyl groups
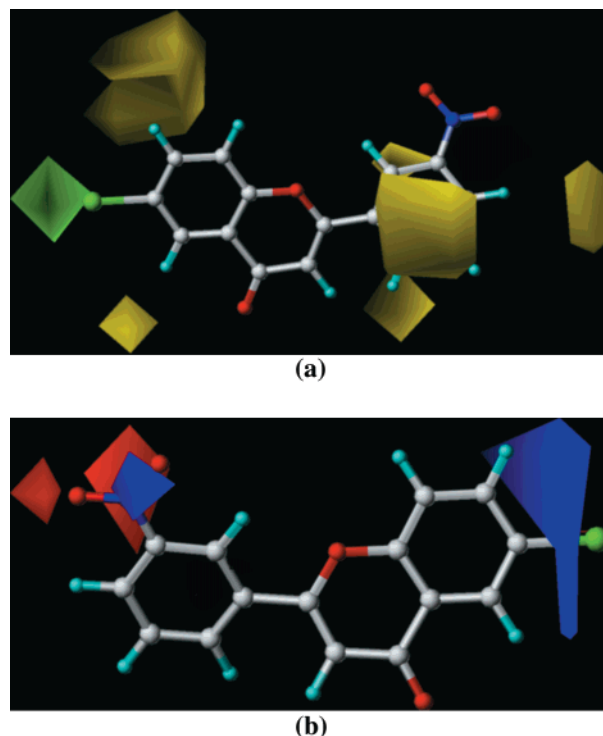
in compounds **33−38** (Table 1) or other large groups at position 5, such as baicalin, baicalein, and scutellarein, have lower binding affinities than other analogues. Introducing any large group, especially at positions 4′, 5′, and 6′, will dramatically decrease the $-\log K_i$ values of flavonoids. This is the reason that there is a sequential $-\log K_i$ value for the compounds: **6** > **7** > **9** > **8**, **32** > **31** > **24** > **20** > scutellarein (Table 1).

1.2. CoMSIA. By use of steric, electrostatic, hydrogen bonding, and hydrophobicity as descriptors, CoMSIA analysis was performed. The results are summarized in Table 4. The predicted binding affinities derived from CoMSIA analysis was also compiled in Table 3 and shown in Figure 2b. The best r_{cross}^2 was found using four descriptor variables. This demonstrates that these variables are necessary to fully describe the field properties around the flavonoid molecules. It also indicates the interaction mode of flavonoids with GABA$_A$ receptors. The steric field explains only 28.1% of the variance, and the additional hydrophobic field explains 23.3% of

Table 5. HQSAR Results for the Flavonoids

no. of compds	cross-validated		conventional		
	q_{cross}^2	optimal components	r^2	s	best length
38	0.751	5	0.968	0.155	59
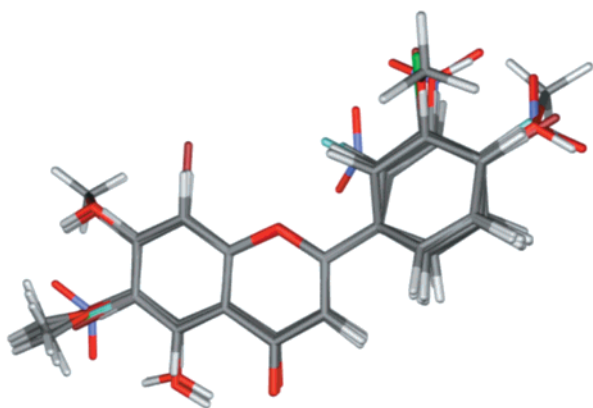
Figure 4. Possible binding conformations of flavonoid derivatives superimposed on the structural template, flavone. This picture is rendered in POV-Ray software[26]

the variance. Thus, the CoMFA steric field can be seen as a comprehensive contribution of the pure steric and hydrophobic effects because the steric contribution of CoMFA is 53.5% (Table 2), which is approximately equal to the summation of the steric and hydrophobic contributions of CoMSIA (51.4%). From the conventional r^2 values (Table 4), it could be found that the electrostatic effect has more contribution to the binding affinities of flavonoids at the BZ site than other factors do.

1.3. HQSAR. Table 5 summarizes the results of the HQSAR calculation. The least standard error occurs at a cross-validated r^2 (q^2) of 0.751 with five optimal components. The hologram that gives the lowest standard error has a length of 59. The PLS analysis yields a conventional r^2 of 0.968 and a standard error s of 0.155 for all the studied compounds. The predicted results are listed in Table 3, and the correlation of the HQSAR predicted values vs the experimental data is presented graphically in Figure 2c. It is important to have a QSAR technique that offers not only a consistent and reproducible prediction but also a fast and convenient procedure. These results indicate that HQSAR is fairly capable of predicting the binding affinities of flavonoids accurately and quickly.

All the statistical data demonstrated that the 3D-QSAR models of flavonoids were stable and predictive, so the 3D-QSAR models have the ability to predict the binding affinity of other flavone analogues. Four compounds, which were reported in our previous paper[21] and not included in the process of the construction of the above QSAR models, were selected to test the predicting capability. The results are also shown in Table 3 and Figure 2, and the predicted $-\log K_i$ values are consistent with the experimental data in the tolerable error range.

2. Mode of Interaction with GABA$_A$ Receptors.
2.1. Pharmacophore. Figure 4 represents the possible binding conformations of the 38 flavonoids predicted from 3D-QSAR models. Figure 5 demonstrates the possible pharmacophore model derived from the
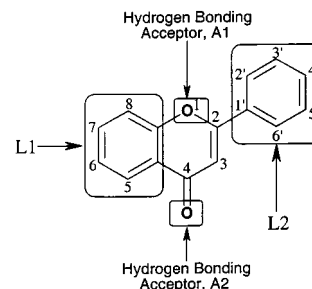
Figure 5. Flavonoids pharmacophore.

CoMFA, CoMSIA, and HQSAR studies. Basically, the key elements of the pharmacophore model are composed of at least two hydrogen bond acceptors labeled as A1 and A2 and two hydrophobic groups labeled as L1 and L2 in Figure 5. Considering the high sensitivity to the substituents at positions 6 and 7, such as for compound **4** compared with **2**, compound **6** compared with **5** (Table 1), and baicalein compared with baicalin, we speculate that there may be two subsites near the L1 site in the GABA$_A$ receptors interacting with flavonoids. These two subsites (labeled S1 and S2) correspond to the steric and electrostatic properties of substituent groups at positions 6 and 7 on the basic skeleton of flavonoids.

In fact, a comprehensive pharmacophore model for ligands binding at the BZ site based on structure−activity relationship studies for structurally different classes of compounds had been developed by Cook and co-workers,[22] and a more recently established pharmacophore for three GABA$_A$/BZ subtypes via SAR study revealed binding differences among receptor subtypes.[23] These models have successfully been employed in the design of novel BZ ligands.[24] When the model for flavonoids herein is compared with those models, the two hydrogen bond acceptor sites are almost the same; A1 (Figure 5) corresponds to H1 in Cook's model, and A2 (Figure 5) corresponds to H2. L1 in Figure 5 looks like L$_{Di}$ in Cook's model or L1 in others,[25] and L2 in Figure 5 occupies a space similar to that of L2 in Cook's model. As for S1 and S2 sites, they are more distinctly related to the specific position for different substituents.

2.2. MO Feature and ESP Mapping. The pharmacophore model proposed above could be further justified by the quantum chemistry calculation study. Two representative compounds, flavone (**1**) and 6-bromo-3′-nitroflavone (**32**) (Table 1), were calculated using the ab initio Hartree−Fock SCF method with the standard polarized double-ζ basis set 6-31G**(HF/6-31G**). To obtain accurate total energies and the orbital features of the binding conformations, the geometries of **1** and **32** were optimized with HF/6-31G** in the constraint of torsion angle $\varphi = 0°$ and $-29.6°$ (corresponding to the torsion angle of the possible binding conformation of **1** and **32**, respectively). The frequency calculation showed that each of the above optimized structure has one negative frequency, indicating that the possible binding conformations are not true local energy-minimum structures. Typically, the conformation representing the pharmacophore is not always the energy minimum; however, it may be at or near a local energy-minimum conformation. We therefore released the constraints and performed a full optimization for compounds **1** and **32**, employing HF/6-31G**. The results
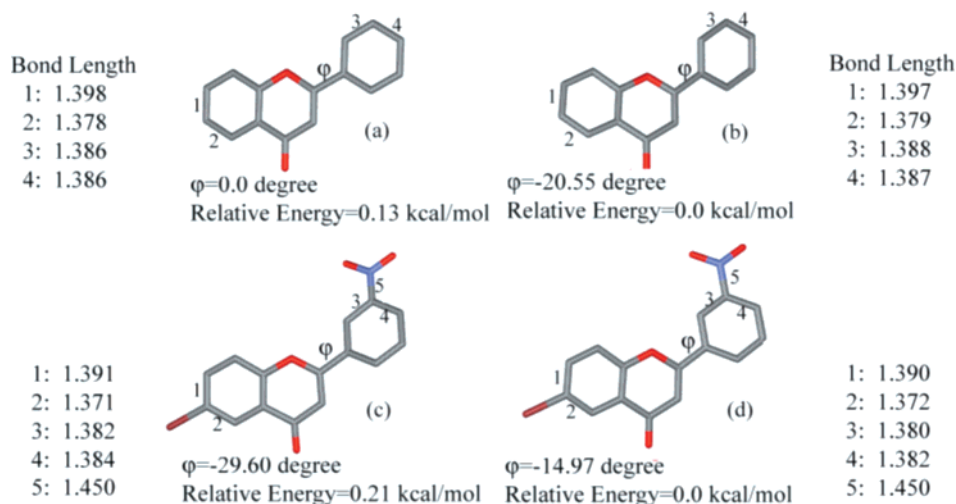
Bond Length
1: 1.398
2: 1.378
3: 1.386
4: 1.386

φ=0.0 degree
Relative Energy=0.13 kcal/mol

Bond Length
1: 1.397
2: 1.379
3: 1.388
4: 1.387

φ=-20.55 degree
Relative Energy=0.0 kcal/mol

1: 1.391
2: 1.371
3: 1.382
4: 1.384
5: 1.450

φ=-29.60 degree
Relative Energy=0.21 kcal/mol

1: 1.390
2: 1.372
3: 1.380
4: 1.382
5: 1.450

φ=-14.97 degree
Relative Energy=0.0 kcal/mol

Figure 6. Energetic and geometric parameters of the binding conformations and corresponding local energy-minimum conformations of flavone (a, b) and nitroflavone (c, d). The structures were optimized, and the energies were calculated with the HF/6-31G** method. The structural picture is rendered in POV-Ray software.[26]
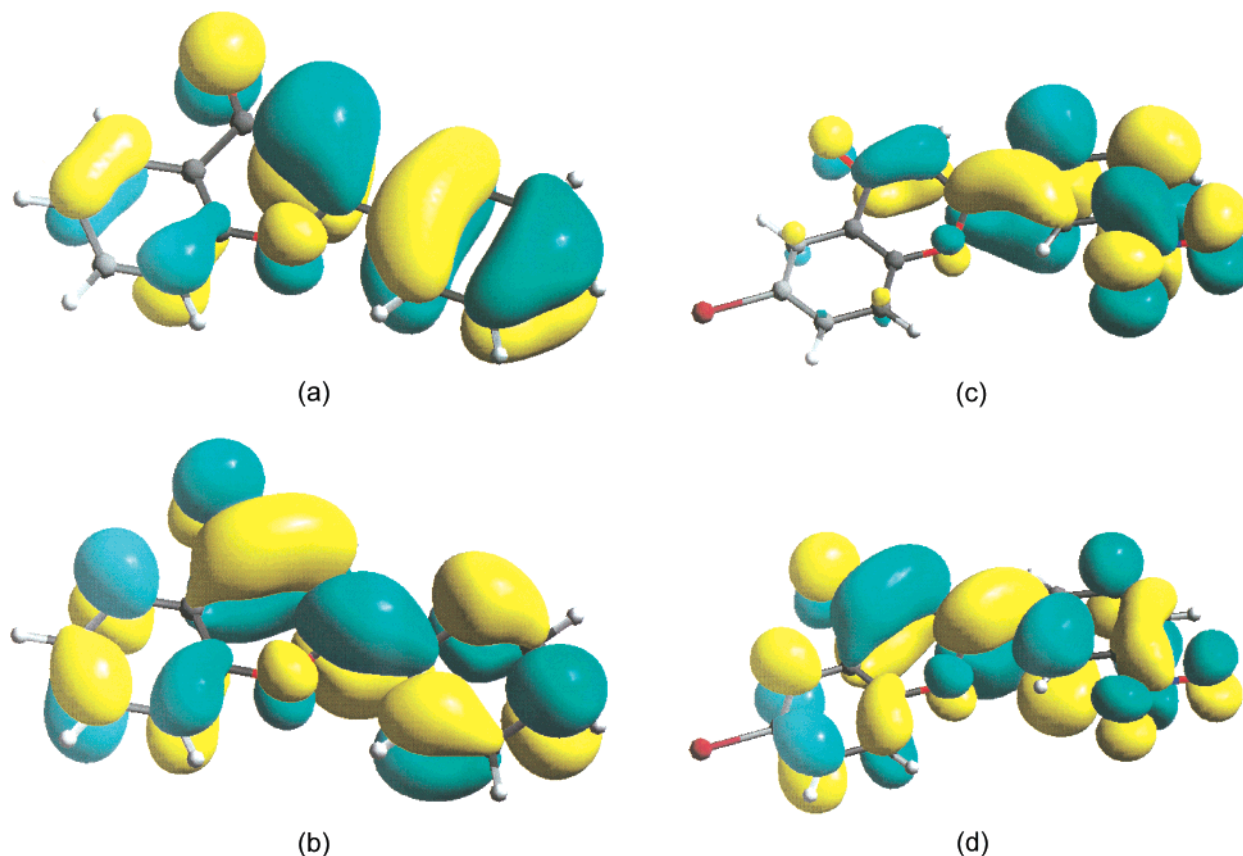
Figure 7. Frontier molecular orbitals of flavone and 6-bromo-3′-nitroflavone: (a) HOMO of flavone; (b) LUMO of flavone; (c) HOMO of 6-bromo-3′-nitroflavone; (d) LUMO of 6-bromo-3′-nitroflavone.

indicated that no negative frequency exists in the fully optimized structures. No obvious differences of HOMO and LUMO were found in fully optimized structures compared with those of the constrained optimized ones for compounds **1** and **32**, respectively. The HF/6-31G** optimized results for both constrained and unconstrained structures are shown in Figure 6. The total energies of the possible binding conformations of compounds **1** (Figure 6a) and **32** (Figure 6c) are only 0.13 and 0.21 kcal/mol higher than those of their local energy minima (parts b and d of Figure 6), respectively. The

bond lengths of the constrained structures almost have no change compared to those of the fully optimized structures (Figure 6). The torsion angle (φ) differences between the possible binding conformations of these two compounds and their local energy minima are respectively about 20° and 15°. Superimposing the possible binding conformation with the local energy-minimum conformation, we found the root-mean-square deviation (rmsd) values are 0.108 for compound **1** and 0.123 for compound **32**. These results demonstrate that the possible binding conformations of **1** and **32** derived from
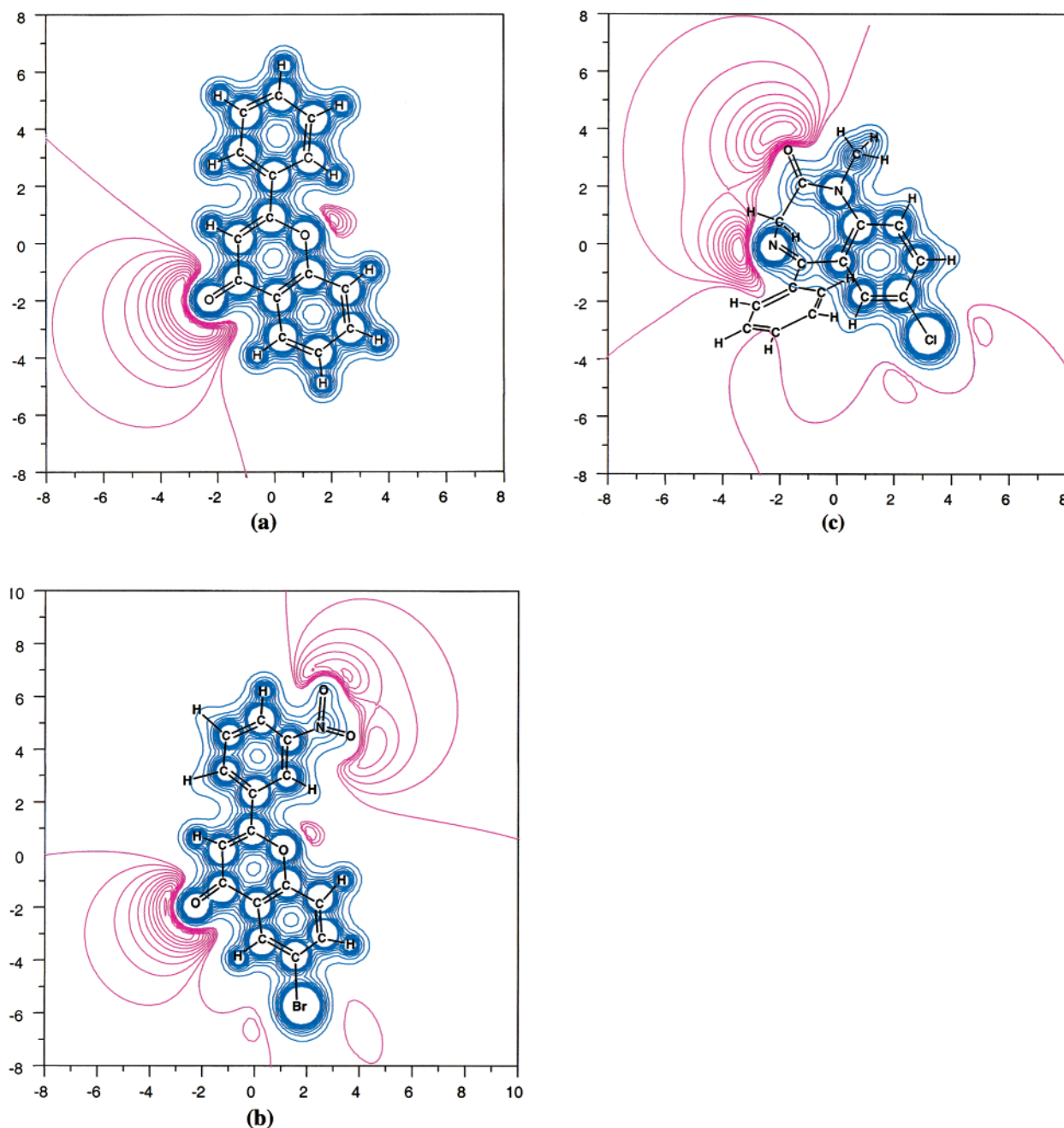
Figure 8. Electrostatic potential maps of flavone (a), 6-bromo-3'nitroflavone (b), and diazepam (c) derived from ab initio HF/6-31G** calculations. The blue lines represent the positive part, and the pink lines represent the negative part. The contour spacing is 0.15 au for the positive part and 0.01 au for the negative part. The units of the axes are in angstroms.

the 3D-QSAR analyses are reasonable because these conformations are near one local energy-minimum conformation.

The geometry of the frame of flavone is hardly influenced by the introduction of either the nitro group at the third position or the bromine at the sixth position. Typically, the changes in the atomic bond distances near the substituted positions are less than 0.01 Å. However, introducing a nitro group in aromatic ring B (Figure 5) leads to a crucial change in the HOMO of compound **32** compared with that of compound **1**, as can be seen from Figure 7. The HOMO of compound **32** is mainly located on aromatic ring B and the nitro group, while the HOMO of compound **1** is more evenly distributed over the whole molecule. On the other hand, the LUMOs of

both compounds are very similar. The fact that compound **32** has a higher binding affinity than compound **1** suggests the importance of the HOMO in the $\pi-\pi$ stacking or hydrophobic interactions. This also implies that the orbital interaction between the flavonoids and the aromatic or some other side chains of residues of GABA$_A$ receptors is dominated by the $\pi-\pi$ or hydrophobic interaction between the HOMO of flavonoids and the LUMO of these residues.

The ESP of compounds **1** and **32** were derived from the HF/6-31G** results, which are shown in Figure 8. The presence of a nitro group introduces great changes in the ESP around the far end of the aromatic ring B. The negative part of the ESP around the nitro group of compound **32** seems to further intensify the interactions

between compound **32** and the active site of GABA$_A$ receptors. The effect of the bromine at the sixth position of flavone is clearly in favor of the electrostatic interaction between the flavone and the S2 subsite of L1 in GABA$_A$ receptors (Figure 5). This has been demonstrated in the lower part of the ESP map of compound **32**, where the negative electrostatic potential around the bromine is obvious. A positively charged side chain of amino acids seems to be arranged near that area in GABA$_A$ receptors. It is important to note that, in Figure 8, the ESP around the oxygen atom of carbonyl group of compound **32** has no significant change compared with that of compound **1**. Therefore, hydrogen bonding between the oxygen and the hydroxyl group containing residues is unaffected by the introduction of the bromine at the sixth position of flavone. Combined with the experimental measurement of the binding affinities of flavonoids (Table 1), theoretical calculations suggest that to achieve high binding affinity the substitutents in the sixth position of flavonoids should maintain the ESP around the oxygen atom of the carbonyl group.

To demonstrate the ability of ESP in mapping the binding site of GABA$_A$ receptors, ab initio calculations were also performed on the classical BZ ligand diazepam and the ESP map was compiled in Figure 8c. Compared with the ESP maps of compounds **1** (Figure 8a) and **32** (Figure 8b), a similar potential feature was found in diazepam (Figure 8c). The negative areas of ESP around the chlorine atom and the C−N=C moiety in diazepam may align respectively with the negative potentials around the bromine atom and the carbonyl group in compounds **1** and **32**. Therefore, these two parts of diazepam may also bind to the GABA$_A$ receptors through electrostatic interaction or hydrogen bonding. A great difference exists for the other parts of the potential of diazepam from that of compounds **1** and **32**, especially the ESP around the methyl group, which is positive. However, the corresponding part (nitro group) of compound **32** is negative. From these we can reveal the binding difference between flavonoids and diazepam in both binding feature and binding affinity.[5,9]

2.3. Interaction Model. Site-directed mutations of GABA$_A$ receptors containing subunit α1 have shown that Tyr161, Thr206, and Phe77 (in γ subunit) residues are involved in the agonist binding.[27−29] Furthermore, progressive deletion experiments have also delineated a membrane-proximal β-rich domain in the GABA$_A$ receptors;[30] this β-strand fragment contains key ligand-binding residues including Tyr161, Thr162, Gly200, Thr206, and Val211 in the α1 subunit.[31,32] A recent study,[33] using the site-directed mutagenesis strategy for the α1 subunit, demonstrated that the amino acid residues of Thr162, Gly200, and Ser204 compose a BZ binding pocket. Ser204 in the α1 subunit probably forms a hydrogen bond in the BZ binding pocket with flavone-like ligands such as zolpidem and CL218872. Taking into account of all these molecular biology studies[27−33] and molecular modeling results,[22−25] a plausible interacting model of flavonoids with the BZ site could be illustrated (Figure 9). One oxygen atom in flavonoids could form a hydrogen bond with the side chains of residues such as Tyr or Thr. The carbonyl oxygen may act as an acceptor in a hydrogen bond formed with the side chains of residues containing a hydroxyl group.
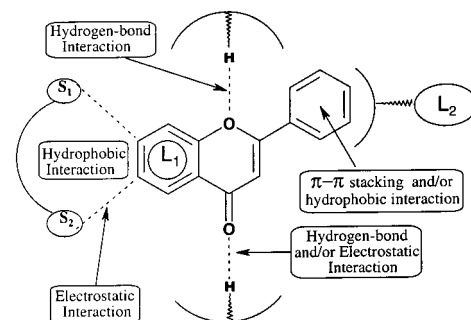

Figure 9. Schematic representation of possible interacting mode of flavonoids at the BZ site in GABA$_A$ receptors.

Some aromatic side chains such as Tyr or hydrophobic residues may interact with flavonoids through π−π stacking and/or hydrophobic interaction. The aromatic side chains in the binding pocket may have strict geometrical orientation, thus making these hydrophobic sites very sensitive to the structural properties of the substituents on aromatic rings A and B (Figure 9).

Conclusions

We have developed predictive 3D-QSAR models of flavonoids through advanced techniques CoMFA, CoMSIA, and HQSAR. Results indicate that the 3D-QSAR models could predict binding affinities of flavonoid analogues within a structurally limited range and enable us to find potent ligand binding at the BZ site in GABA$_A$ receptors. In addition, the 3D-QSAR results provide a reasonable pharmacophore model for the flavonoids. The precise ab initio calculations on the constrained and unconstrained structures of compounds **1** and **32** have verified the binding conformations and the pharmacophore model of flavonoids. The ESP maps provide an additional concrete indication for the pharmacophore; i.e., electrostatic interaction may exist between the L1 moiety of flavonoids and the S2 subsite of the receptors (Figure 9). This proposed mode of interaction for flavonoids with GABA$_A$ receptors may offer some important clues for paving the way to the eventual identification of relevant pharmacophoric sites in the receptor, such as replacing the negatively charged amino acid residues with positively charged ones in the subsite S2 through site-directed mutagensis, which may increase the binding affinity of the ligands to GABA$_A$ receptors.

References

(1) Medina, J. H.; Viola, H.; Wolfman, C.; Marder, M.; Wasowski, C.; Calvo, D.; Paladini, A. C. Overview−Flavonoids: A new family of benzodiazepine receptor ligands. *Neurochem. Res.* **1997**, *22*, 419−425.
(2) Marder, M.; Viola, H.; Wasowski, C.; Wolfman, C.; Waterman, P. G.; Cassels, B. K.; Medina, J. H.; Paladini, A. C. 6-Bromoflavine, a high affinity ligand for the central benzodiazepine receptors is a member of a family of active flavonoids. *Biochem. Biophy. Res. Commun.* **1996**, *223*, 384−389.
(3) Marder, M.; Zinczuk, J.; Colombo, M. I.; Wasowski, C.; Viola, H.; Wolfman, C.; Medina, J. H.; Ruveda, E. A.; Paladini, A. C. Synthesis of halogenated flavone derivatives and evaluation of their affinity for the central benzodiazepine receptors. *Bioorg. Med. Chem. Lett.* **1997**, *7*, 2003−2008.

(4) Marder, M.; Viola, H.; Bacigaluppo, J. A.; Colombo, M. I.; Wasowski, C.; Wolfman, C.; Medina, J. H.; Ruveda, E.; Paladini, A. C. Detection of benzodiazepine receptor ligands in small libraries of flavone derivatives synthesized by solution phase combinatorial chemistry. *Biochem. Biophy. Res. Commun.* **1998**, *249*, 481−485.

(5) Teuber, L.; Watjen, F.; Jensen, L. H. Ligands for the benzodiazepine binding site—a survey. *Curr. Pharm. Des.* **1999**, *5*, 317−343.

(6) Argyropoulos, S. V.; Nutt, D. The use of benzodiazepines in anxiety and other disorders. *Eur. Neuropsychopharmacol.* **1999**, Suppl 6, s407−s412.

(7) McKernan, R. M.; Whiting, P. Which GABA$_A$-receptor subtypes really occur in the brain? *TINS* **1996**, *19*, 139−143.

(8) Viola, H.; Marder, M.; Wolfman, C.; Wasowski, C.; Medina, J. H.; Paladini, A. C. 6-Bromo-3′-nitroflavone, a new high affinity benzodiazepine receptor agonist recognizes two populations of central cortical binding sites. *Bioorg. Med. Chem. Lett.* **1997**, *7*, 373−378.

(9) Wang, Q. M.; Han, Y. F.; Xue, H. Ligands of the GABA$_A$ receptor benzodiazepine binding site. *CNS Drug Rev.* **1999**, *5*, 125−144.

(10) Da Settimo, A.; Primofiore, G.; Da Settimo, F.; Marini, A. M.; Novellino, E.; Greco, G.; Martini, C.; Giannaccini, G.; Lucacchini, A. Synthesis, structure−activity relationships, and molecular modeling studies of N-(indol-3-ylglyoxylyl)-benzylamine derivatives acting at the benzodiazepine receptor. *J. Med. Chem.* **1996**, *39*, 5083−5091.

(11) Dekermendjian, K. P.; Witt, M. R.; Sterner, O.; Nielsen, M.; Liljefors, T. Structure−activity relationships and molecular modeling analysis of flavonoids binding to the benzodiazepine site of the rat brain GABA$_A$ receptor complex. *J. Med. Chem.* **1999**, *42*, 4343−4350.

(12) Diaz-Arauzo, H.; Evoniuk, G. E.; Skolnick, P.; Cook, J. M. The agonist pharmacophore of the benzodiazepine receptor. Synthesis of a selective anticonvulsant/anxiolytic. *J. Med. Chem.* **1991**, *34*, 1754−1756.

(13) Zhang, W.; Koehler, K. F.; Zhang, P.; Cook, J. M. Development of a comprehensive pharmacophore model for the benzodiazepine receptor. *Drug Des. Dev.* **1995**, *12*, 193−248.

(14) Cox, E. D.; Diaz-Arauzo, H.; Huang, Q.; Reddy, M. S.; Ma, C.; Harris, B.; McKernan, R.; Skolnick, P.; Cook, J. M. Synthesis and evaluation of analogues of the partial agonist 6-(propyloxy)-4-(methoxymethyl)-β-carboline-3-carboxylic acid ethyl ester (6-PBC) and the full agonist 6-(benzyloxy)-4-(methoxymethyl)-β-(carboline-3-carboxylic acid ethyl ester (Zk93423) at wild type and recombinant GABA$_A$ receptors. *J. Med. Chem.* **1998**, *41*, 2537−2552.

(15) Cramer, M.; Cramer, R. D., III; Jones, D. M. Comparative molecular field analysis. 1. effect of shape on binding of steroids to carrier proteins. *J. Am. Chem. Soc.* **1988**, *110*, 5959−5967.

(16) Klebe, G.; Abraham, U.; Mietzner, T. Molecular similarity indices in a comparative analysis(CoMSIA) of drug molecules to correlate and predict their biological activity. *J. Med. Chem.* **1994**, *37*, 4130−4146.

(17) Tong, W.; Lowis, D. R.; Perkins, R.; Chen, Y.; Welsh, W. J.; Goddette, D. W.; Heritage, T. W.; Sheehan, D. M. Evaluation of quantitative structure−activity relationship methods for large-scale prediction of chemicals binding to the estrogen receptor. *J. Chem. Inf. Comput. Sci.* **1998**, *38*, 669−677.

(18) Frisch, M. J.; Trucks, G. W.; Schlegel, H. B.; Scuseria, G. E.; Robb, M. A.; Cheeseman, J. R.; Zakrzewski, V. G.; Montgomery, J. A., Jr.; Stratmann, R. E.; Burant, J. C.; Dapprich, S.; Millam, J. M.; Daniels, A. D.; Kudin, K. N.; Strain, M. C.; Farkas, O.; Tomasi, J.; Barone, V.; Cossi, M.; Cammi, R.; Mennucci, B.; Pomelli, C.; Adamo, C.; Clifford, S.; Ochterski, J.; Petersson, G. A.; Ayala, P. Y.; Cui, Q.; Morokuma, K.; Malick, D. K.; Rabuck, A. D.; Raghavachari, K.; Foresman, J. B.; Cioslowski, J.; Ortiz, J. V.; Stefanov, B. B.; Liu, G.; Liashenko, A.; Piskorz, P.; Komaromi, I.; Gomperts, R.; Martin, R. L.; Fox, D. J.; Keith, T.; Al-Laham, M. A.; Peng, C. Y.; Nanayakkara, A.; Gonzalez, C.; Challacombe, M.; Gill, P. M. W.; Johnson, B. G.; Chen, W.; Wong, M. W.; Andres, J. L.; Head-Gordon, M.; Replogle, E. S.; Pople, J. A. *Gaussian 98*; Gaussian, Inc.: Pittsburgh, PA, 1998.

(19) *Sybyl*, version 6.5; Tripos Associates: St. Louis, MO, 1998.

(20) Ghose, A. K.; Viswanadhan, V. N.; Wendoloski, J. J. A knowledge-based approach in designing combinatorial or medicinal chemistry libraries for drug discovery. 1. A qualitative and quantitative characterization of known drug databases. *J. Comb. Chem.* **1999**, *1*, 55−68.

(21) Hui, K. M.; Wang, X. H.; Xue, H. Interaction of flavones from the roots of *Scutellaria baicalensis* with the benzodiazepine site. *Planta Med.* **2000**, *66*, 91−93.

(22) Zhang, W.; Koehler, K. F.; Zhang, P.; Cook, J. M. Development of a comprehensive pharmacophore model for the benzodiazepine receptor. *Drug Des. Dev.* **1995**, *12*, 193−248.

(23) Huang, Q.; He, X. H.; Ma, C. R.; Liu, R. Y.; Yu, S.; Dayer, C. A.; Wenger, G. R.; McKernan, R.; Cook, J. M. Pharmacophore/receptor models for GABA$_A$/BzR subtypes ($\alpha1\beta3\gamma2$, $\alpha5\beta3\gamma2$, and $\alpha6\beta3\gamma2$) via a comprehensive ligand-mapping approach. *J. Med. Chem.* **2000**, *43*, 71−95.

(24) Cox, E. D.; Diaz-Arauzo, H.; Huang, Q.; Reddy, M. S.; Ma, C.; Harris, B.; McKernan, R.; Skolnick, P.; Cook, J. M. Synthesis and evaluation of analogues of the partial agonist 6-(propyloxy)-4-(methoxymethyl)-β-carboline-3-carboxylic acid ethyl ester (6-PBC) and the full agonist 6-(benzyloxy)-4-(methoxymethyl)-β-(carboline-3-carboxylic acid ethyl ester (Zk93423) at wild type and recombinant GABA$_A$ receptors. *J. Med. Chem.* **1998**, *41*, 2537−2552.

(25) Huang, Q.; Cox, E. D.; Gan, T.; Ma, C.; Bennett, d. W.; McKernan, R. M.; Cook, J. M. Studies of molecular pharmacophore/receptor models for GABA$_A$/benzodiazepine receptor subtypes: Binding affinities of substitutes β-carboline ligands for $\alpha x\beta3\gamma2$ (x = 1 − 3, 5, 6) subtypes and quantitative structure−activity relationship studies via comparative molecular field analysis. *Drug Des. Discovery* **1999**, *16*, 55−76.

(26) *POV-ray-Team*; POV-ray, version 3; 1999 (www.povray.org).

(27) Buhr, A.; Baur, R.; Malherbe, P.; Sigel, E. Point mutations of the $\alpha1\beta2\gamma2$ γ-aminobutyric acid A receptor affecting modulation of the channel by ligands of the benzodiazepine binding site. *Mol. Pharmacol.* **1996**, *49*, 1080−1084.

(28) Buhr, A.; Schaerer, M. T.; Baur, R.; Sigel, E. Residues at positions 206 and 209 of a1 subunit of γ-aminobutyric acid A receptors influence affinities for benzodiazepine binding site ligands. *Mol. Pharmacol.* **1997**, *52*, 672−682.

(29) Jursky, F.; Fuchs, K.; Buhr, A.; Tretter, V.; Sigel, E.; Sieghart, W. Identification of amino acid residues of GABA(A) receptor subunits contributing to the formation and affinity of the tert-butylbicyclophosphorothionate binding site. *J. Neurochem.* **2000**, *74*, 1310−1316.

(30) Xue, H.; Chu, R. A.; Hang, J.; Lee, P.; Zheng, H. Fragment of GABA$_A$ receptor containing key ligand-binding residues over-expressed in *Escherichia coli*. *Protein Sci.* **1998**, *7*, 216−219.

(31) Xue, H.; Huang, J.; Chu, R. A.; Xiao, Y. Z.; Li, H. M.; Lee, P.; Zheng, H. Delineation of a membrane-proximal β-rich domain in the GABA$_A$ receptor by progressive deletions. *J. Mol. Biol.* **1999**, *285*, 55−61.

(32) Xue, H.; Zheng, H.; Li, H. M.; Kitmitto, A.; Zhu, H.; Lee, P.; Holzenburg, A. A fragment of recombinant GABA(A) receptor alpha1 subunit forming rosette-like homo-oligomers. *J. Mol. Biol.* **2000**, *296*, 739−742.

(33) Renard, S.; Olivier, A.; Granger, P.; Avenet, P.; Graham, D.; Sevrin, M.; George, P.; Besnard, F. Structural elements of the γ-aminobutyric acid type a receptor conferring subtype selectivity for benzodiazepine site ligands. *J. Biol. Chem.* **1999**, *274*, 13370−13374.

JM000557P